RSC Advances




ROYAL SOCIETY OF CHEMISTRY

www.rsc.org/advances

# Microencapsulation of Ammonium Polyphosphate with Melamine-formaldehyde-tris(2-hydroxyethyl) Isocyanurate Resin and its Flame Retardancy in Polypropylene

Ziwei Jiang and Gousheng Liu*

*State Key Laboratory of Chemical Engineering, East China University of Science and Technology, Shanghai 200237, China.*

**Abstract**: Microencapsulated ammonium polyphosphate with a novel melamine-formaldehyde-tris(2-hydroxyethyl) isocyanurate resin (MFT resin) was prepared by in situ polymerization. This microencapsulated ammonium polyphosphate was named MFT-APP. The MFT resin and MFT-APP were characterized by FTIR, XPS, TGA and SEM. Polypropylene(PP)/MFT-APP and PP/MFT-APP/THEIC were prepared. Their thermal stability and flame retardancy were investigated through TGA, limiting oxygen index (LOI), vertical burning test and cone calorimeter test. SEM was used again to observe the morphology of char residues. The results illustrated that MFT-APP and MFT-APP/THEIC had excellent flame retardant properties on PP. Furthermore, Water resistant test demonstrated that PP/ MFT-APP/THEIC had better flame durability than PP/APP/THEIC. TGA-FTIR and XPS results revealed that the efficient flame retardancy of MFT-APP/THEIC was mainly attributed to the formation of a compact and thermostable intumescent char on underlying materials during a fire.

**Keywords:** Melamine-formaldehyde-tris(2-hydroxyethyl) isocyanurate resin; Tris(2-hydroxyethyl) isocyanurate (THEIC); Microencapsulated ammonium polyphosphate; flame retardancy; Polypropylene (PP).

Corresponding author:

Tel: +86-21-33612485 E-mail: gsliu@ecust.edu.cn (Gousheng Liu)

## 1. Introduction

With the development of materials science, polymer materials receive a high speed development. As one of the widely used polymer materials, polypropylene (PP) has outstanding features such as low price, low density, non-toxic, easy processing and excellent mechanical properties, so it can be used as electrical, building, transport applications and general household materials[1-2]. However, its inherent high flammability and melt dripping drawbacks limit its application range. Therefore, it is essential to endow PP with good flame retardancy[3].

In recent years, intumescent flame retardants (IFRs) have drawn much attention due to their halogen-free, low toxicity, low smoke production and anti-dropping characteristics [4-5]. Generally, a typical IFR system is composed of three components: an acid resource, a charring agent and a blowing agent[6-8]. The acid resource is generally inorganic acid or precursor of acid, for example, ammonium polyphosphate (APP)[9]. During the combustion process, APP can release the $NH_3$ and the inorganic acid, and then there is a esterification reaction between the inorganic acid and the charring agent . At last it will form a intumescent charred layer cover on the surface of the polymer materials[10-12]. During materials processing, workers find that APP is easily exuded to the surface of materials, resulting in a decrease of flame-retardant efficiency[13-14]. Furthermore, APP has a low compatibility with polymer materials, affecting mechanical properties of polymeric composites[15-16]. Modification of APP with surfactants or microencapsulating with water-insoluble polymers are effective methods to improve water resistance and the polarity of APP[17-18] . Melamine–formaldehyde (MF) resin is widely used as coating materials for modification. For example, Wu[19] studied the flame retardancy of microencapsulated

ammonium polyphosphate with MF resin on PP, he found that the particles' size and water absorption of MFAPP was decreased. Yang[20] studied the thermal stability and the flame retardancy of PP/MF-APP/pentaerythritol(PER) system, he found that MF-APP was beneficial for improving the thermal stability and flame retardancy of PP/MF-APP/PER composites. However, researchers also found that APP or MF-APP used alone in PP cannot reach UL-94 V-0 rating at 30% dosage[19,21]. Incorporating an effective charring agent into the coating materials will be a promising route.

Tris(2-hydroxyethyl) isocyanurate (THEIC) was mainly used to prepare the polyester-based heat-resisting insulating paint. THEIC also could be a modifier for MF resin which could improve the flexibility and cohesiveness of MF resin[22-24]. As a derivative of triazine compound, THEIC and its derivatives could be served as the charring agent. Bourbigot[25] found that there was a synergistic effect between APP and THEIC. Chen[26] studied the advantages and disadvantages of THEIC when it was served as a charring agent. Yuan[27]and Chen[28] synthesized a novel charring agent tris(2-hydrooxyethyl) isocyanurate terephthalic acid ester, this charring agent exhibited high flame retardant efficiency on polylactide (PLA) and PP. Theoretically, introducing THEIC into MF resin as the coating materials for APP will be a novel route for improving the water resistance, thermal stability and flame retardancy of APP. In this work, MFT resin was prepared by in situ polymerization and it was characterized by Fourier transform infrared (FTIR). Then MFT resin was used as the coating material for APP. The structure and thermal property of MFT-APP were characterized by FTIR, X-ray photoelectron spectroscopy (XPS), thermogravometric analysis (TGA) and scanning electron microscope (SEM). The MFT-APP and MFT-APP/THEIC were added into PP, measurements such as TGA, LOI, vertical burning test (UL-94) and cone calorimeter test were used. The morphology of char

residues were observed by SEM. Water resistance of the flame retardant composites was investigated. TGA-FTIR and XPS were used to analysis the thermal degradation of flame retardant composites.

## 2 Experimental Section

### *2.1 Materials*

Polypropylene ( PP, isotactic, T30s, melt-flow rate:2.3g/10min) was supplied by SINOPEC Maoming Company, China. Ammonium polyphosphate (APP) with average particle size 10μm was purchased from Shandong Shi'an Chemical Co., Ltd. THEIC was purchased from Changzhou Lantian Chemical Co., Ltd. Melamine was obtained from Sinopharm Chemical Reagent Co., Ltd. Formaldehyde solution (mass fraction 36%) was obtained from Meryer (Shanghai) Chemical Technology Co., Ltd. Anhydrous sodium carbonate ($Na_2CO_3$) was obtained from Tianjian Zhiyuan Chemical Reagents, China. Acetic acid was purchased from Sinopharm Chemical Reagent Co., Ltd. All reagents were used as received.

### *2.2 Preparation of Microencapsulated APP*

Preparation of the MFT resin pre-polymer: 37% formaldehyde solution and melamine (with a mole ratio of 3:1) were added into a four-neck bottle with a stirrer. The mixture was adjusted to pH 8–9 with 10% $Na_2CO_3$ solution, heated to about 95 °C and kept at that temperature for 0.5 h. When the mixture turned into transparent, the suitable amount of THEIC was put into the mixture and kept at 95 $^{o}$C for another 1 h. The MFT pre-polymer solution was prepared. Figure 1 shows reaction scheme.

Preparation of microencapsulated APP: APP (100 g) was first dispersed in 200 ml ethanol. Then suitable amount of MFT pre-polymer solution (coating rate is 30%) was added into the suspension, the pH of the mixture was adjusted to 4–5 with acetic

acid. The resulting mixture was heated at 80 $^{o}$C for 2 h. Then, the mixture was cooled to room temperature, filtered, washed with distilled water, and dried at 100 $^{o}$C. The MFT-APP powder was finally obtained.

(inserting figure 1 here)

*2.3 Preparation of flame- retardant PP samples*

All samples were prepared via melt compounding at 180°C in an internal mixer(SU70, Suyan Technology Company, China) with a rotate speed of 20 rpm for 8-10 minutes for each sample. The resulting composites were dried in an oven, and then molded into testing bars with plate vulcanization machine for fire property characterization.

*2.4 Characterization*

FTIR spectra of the samples were recorded on a Bruker-Vertex 70 FTIR spectrometer in the range of 400-4000 $cm^{-1}$ by using KBr pellets. The thermogravimetry analysis (TGA) tests were carried out on Diamond TG/DTG (PE, America) at a heating rate of 10 °C /min from room temperature to 800 °C with air atmosphere, sample weight was kept within 10 mg. The X-ray photoelectron spectroscopy (XPS) spectra were recorded with a VG ESCALAB MK II spectrometer using Al Kα excitation radiation ($hv$ =1253.6 eV). Water contact angles were measured with a JC2000C2 contact angle goniometer (Shanghai Zhongchen Powereach Company,China) by the sessile drop method. Limiting oxygen index (LOI) was carried out in an HC-2 oxygen index meter (Jiangning Analysis Instrument Co., China). The vertical burning tests were conducted according to the UL-94 test standard (ASTM D3801) with a test dimensions of 130×13×3 $mm^3$. The morphology

of the residual char obtained from the LOI test was examined by means of field emission scanning electron microscopy (JSM-6360). The surface of residual char was sputter-coated with a gold layer before examination. The combustion properties were evaluated by a cone calorimeter. All samples (100×100×3 $mm^3$) were exposed to a Stanton Redcroft cone calorimeter under a heat flux of 50 $kW/m^2$ according to ISO-5660 standard. Tensile tests were completed in accordance with the procedures in GB/T 1040-1992 at a crosshead speed of 50 mm/min. Flexural properties were carried out in accordance with the procedures in GB/T 9314-2000 at a crosshead speed of 2 mm/min. Thermogravimetry-Fourier transform infrared spectroscopy (TGA-FTIR) was performed using a SDT Q600 V20.5 Build 15 instrument that was interfaced to a Nicolet IS10 FTIR spectrometer. About 5.0 mg of the sample was put in an alumina crucible and heated from 40 to 800 $^oC$. The heating rate was set as 20 $^oC$ /min ( air atmosphere)

## 3 Results and discussion

### *3.1 Characterization of MFT-APP*

#### *3.1.1 Chemical Structure of MFT resin*

(inserting figure 2 here)

FTIR spectra of MF resin and MFT resin were shown in figure 2. For MF resin, the absorption peak at 3332 $cm^{-1}$ was attributed to the stretching vibration of N-H and O-H, or coupled absorption of hydrogen bonds. The peak at 2943 $cm^{-1}$ was attributed to the C-H stretching vibration of $-CH_2$ groups. The absorptions of 1589, 1500, and 1360$cm^{-1}$ were due to the ring vibration of MEL. The spectrum of MFT resin revealed not only well-defined absorption peaks of MF resin, but also the characteristic bands

of THEIC. There were two obvious absorption peaks at 1713 $cm^{-1}$ and 766 $cm^{-1}$, which could be found in the spectrum of MFT resin. They were assigned to the -C=O stretching vibration and triazine ring skeleton vibration. The appearance of these characteristic peaks in THEIC indicated the successful incorporation of THEIC into the MF resin.

*3.1.2 Thermal stability of MF and MFT resin*

(inserting figure 3 here)

The TG and DTG curves of MF and MFT resin are shown in figure 3. MF and MFT resin show a similar decomposing behavior. There were two main decomposing processes for them in air atmosphere: 50-100 $^{o}C$ and 350-400 $^{o}C$ . We supposed the first weight loss is primarily due to water vaporization. The second weight loss is correspond to the structural decomposition of the resins. The maximum weight loss rate of MF resin is larger than MFT resin. The DSC results for MF and MFT resin are shown in figure 4. For them, there is a main endothermic peak at 90 $^{o}C$ , which is correlated with the water vaporization. With the rising of temperature, endothermic situation is declining. Though there is a some small up and downs , we think the lowest point ( about 150 $^{o}C$) may be the curing temperature for MFT resin.

(inserting figure 4 here)

*3.1.3 Chemical Structure of MFT-APP*

(inserting figure 5 here)

The FTIR spectra of APP and MFT-APP were shown in figure 5, the spectrum of MFT resin was added as a contrast. The typical absorption peaks of APP included

3223 $cm^{-1}$ (N–H), 1256 (P=O), 1069 $cm^{-1}$ (P–O asymmetric vibration), 1020 $cm^{-1}$ (symmetric vibration of $PO_2$), 881 $cm^{-1}$ (P–O asymmetric stretching vibration), and 800 $cm^{-1}$ (P–O–P). For the MFT-APP, the main absorption peaks appeared at 3204, 1554, 1419, 1255, 1069, 1020, 880 and 800 $cm^{-1}$. The typical absorption peaks of APP were well verified in the structure of MFT-APP. Meanwhile, the peak at 1554 $cm^{-1}$ and 1419 $cm^{-1}$ were assigned to the ring vibration of MEL from the MF resin. It was clear that not only the absorption peaks of MFT resin but also the characteristic bands of APP appeared on the FTIR spectra of MFT-APP. Above results proved that APP was well coated by the MFT resin.

(inserting figure 6 here)

The XPS spectrum of APP and MFT-APP was shown in figure 6. The peaks located at 134 eV and 192 eV were assigned to the typical chemical shifts of $P_{2P}$ and $P_{2S}$ in APP. For MFT-APP, the intensities of peaks mentioned above decreased sharply, meanwhile the intensities of the $C_{1S}$ peak increases greatly. The intensities of the $N_{1S}$ peak did not increase greatly like the $C_{1S}$ ones, which were attributed to the structure of THEIC in the MFT resin. The growth and decline relationship among these typical chemical shifts eloquently proved that APP was well coated by the MFT resin.

( inserting figure 7 here)

Figure 7 shows the surface morphologies of APP and MFT-APP. The surface of APP particle was very smooth. After APP was microencapsulated by MFT resin, the MFT-APP presented a comparably rough surface . It was evidence that APP was well

coated by the MFT resin. As we know, water contact angle tests could evaluate the surface hydrophobicity of solid powder. As shown in Fig 7, the water contact angle of APP is only 9°. This indicated that pure APP is hydrophibic with high surface energy and easily attacked by the influence of water or moisture. However, due to the formation of the weak polar MFT resin microcapsules on the surface of APP, the hydrophile of MFTAPP is greatly decreased. In this condition, the water contact angle of MAPP reaches 45°. When MFT-APP particles are incorporated into polymer matrix, the compatibility between MFT-APP and polymer materials will be improved.

( inserting table 1 here)

Table 1 shows the solubility of APP and MFT-APP. The solubility of APP was 0.55 g/ 100 ml $H_2O$ at room temperature (25 $^oC$). After APP particles were microencapsulated by the MFT resin, the solubility of MFT-APP was decreased to 0.3 g/ 100 ml $H_2O$. The solubility was decreased about 45.5% after APP was microencapsulated. The results proved that APP was well microencapsulated by MFT resin.

( inserting figure 8 here)

( inserting table 2 here)

The TG and DTG curves of APP, MFAPP and MFT-APP were shown in figure 8 and the corresponding data were listed in table 2. There were two decomposing processes for APP in air atmosphere: 220-460 $^oC$ and 460-800 $^oC$. The temperatures with the maximum mass loss rates during the two steps are 330 $^oC$ and 607 $^oC$,

respectively. The weight loss of the first stage ( 220-460 $^{o}$C) should be attributed to the elimination of $NH_3$ and $H_2O$ in the thermal degradation process of polyphosphate. The weight loss of the second stage ( beyond 460 $^{o}$C) was attributed to the release of phosphoric acid, polyphosphoric acid, and metaphosphoric acid with APP decomposition. However, MFAPP and MFT-APP showed different degradation behavior compared with APP at the whole process. There were about three degradation stages for MFAPP and MFT-APP. The onset decomposition temperature ($T_{5\%}$) and the first maximum weight loss temperature ($T_{max1}$) were shifted to lower temperature. At the first degradation stage, MFAPP and MFT-APP decomposed faster than APP, which can be attributed to the low thermal stability of the MF resin and MFT resin. The weight loss might be caused by the release of the nonflammable gases from the resin. For the second and third degradation stages, it was the results of joint action between APP and the resin. The residual of the resin and the phosphorus-containing compounds would inhibit APP further decomposition. From data listed in table 2, it was clear that the thermal stability of MFT-APP was better than others in the high tmperature. As mentioned above, THEIC can reacted with APP, introducing THEIC into the MF resin would be helpful for improving the thermal stability of APP. Moreover, MFT-APP had about 34.9% residue after 800 $^{o}$C, whereas the residue for APP and MFAPP at this temperature was just 14.5% and 24.2%, respectively. It is clear that MFT-APP presented better thermal stability than APP and MFAPP in the high temperature.

*3.2 Flame retardancy and burning behaviors*

*3.2.1 LOI and UL-94 tests*

(inserting table 3 here)

The LOI and UL-94 tests were listed in the table 3.

It could be found that pristine PP (PP0) was highly combustible and could not reach any UL-94 rating. After 30 wt% APP and MFAPP was added into the PP (PP1 and PP2), the LOI value increased to 21% and 30.5% respectively. However, PP1 and PP2 still could not pass the UL-94 V-0 test owing to the scarcity of charring agent. When 30 wt% MFT-APP was added to PP (PP3), PP3 successfully passed V-0 level of UL-94 test . The reason may contain two aspects, one was the MFT resin released water vapor and $NH_3$ gases which would reduce the concentration of air and make the char swell to form protective char. The other reason can be attributed to the structure of THEIC in the MFT resin, which would enhance the synergistic effect between the phosphorus and nitrogen. Though the MFT-APP/PP could pass the UL-94 V-0 test, the LOI value still be low. In order to further improve the flame retardancy, THEIC was added into the PP/MFT-APP composites, which was served as a charring agent. From the data listed in table 3, it was clear that the LOI values of the ternary composites were increased greatly. At the same additive level (30%), the highest LOI value could obtain 36%. When the total addition of the MFT-APP and THEIC was decreased into 25%, all ternary composites still could obtain UL-94 V-0 rating. These results demonstrated that MFT-APP and MFT-APP/THEIC would remarkably improve flame retardant performance of PP, and THEIC showed a good synergistic effect with

MFT-APP.

*3.2.2 Thermal stability of flame retardant PP*

( inserting figure 9 here)

( inserting table 4 here)

The thermal degradation behavior of PP0, PP2, PP3 and PP6 was shown in figure 9 and the corresponding data were listed in table 4. It could be seen that only one step weight loss ( 300-450 $^{o}$C ) for pure PP (PP0) and the maximum mass loss rate occurred at about 322.5 $^{o}$C. There was a similar thermal decomposition behavior between PP2 and PP3, they had an approximate onset decomposition temperature ($T_{5\%}$) and similar decomposing stages. The thermal stability of PP3 was better than PP2. When THEIC was incorporated into the PP/MFT-APP, the thermal decomposition behavior of the flame retardant composites changed greatly. Before temperature 630 $^{o}$C, PP6 had a lower thermal stability than PP2 and PP3, which could be attributed to the low stability of THEIC. At 287$^{o}$C, the first maximum weight loss was occurred for PP6. The first maximum weight loss rate of PP6 was larger than PP2 and PP3. The reason might be THEIC could promote the decomposition of MFT-APP. After temperature 630 $^{o}$C, the thermal stability of PP6 was better than PP2 and PP3. The reason could be attributed to the synergistic effect between THEIC and MFT-APP. The synergistic effect between THEIC and MFT-APP was benefical for forming a swell char layer , and this swell char layer would protect the below materials from further decomposition.

( inserting figure 10 here)

The residual charred layer was important for the flame retardancy of polymer materials. The images of residual chars for PP1, PP2, PP3 and PP6 were shown in figure 10. As seen in figure 10a, no residual chars could be seen on the surface of PP1. It was attributed to lack of char formation during combustion. Heat and volatiles could easily penetrate the surface during the burning process. For PP2 and PP3, a typical intumescent charring layer still could not be seen, which was due to insufficient charring agent introduced into the system. Though PP3 could pass the UL-94 V-0 test, the incorporation of THEIC into the MF resin was helpful for improving the thermal stability of the MFT-APP. The situation was improved greatly when THEIC served as a charring agent. For PP6, a compact and swelling structure could be observed. Furthermore, there were lots of folds on the surface, which could act as a skeleton to strengthen the surface layer[29-30].

This result provided further evidence that THEIC had a good synergistic effect with the MFT-APP, homogeneous and stable intumescent char layer formed, leading to better flame retardancy.

( inserting figure 11 here)

( inserting figure 12 here)

The digital images of the residual chars for PP0, PP3 and PP6 were shown in figure 11. Nothing was left for PP0 which was coincided with inherent properties of flammability and melt dripping of PP. However, situation was improved to some extent after 30 wt% MFT-APP was added into the PP. For PP3, some swollen residual char could be seen, though the degree of the expansion was not ideal. After THEIC was added into the flame retardant composites, a compact and dense char layer was observed on the external surface of PP6. This swollen charred layer could be

effectively prevented the inside pyrolysis products from transmitting into the flame zone.

The cone calorimeter test was considered to be an effective way to simulate the actual fire burning behavior and the measurements provided several useful burning parameters[31-33].

The HRR and THR curves of PP0, PP3 and PP6 were shown in figure 12 and the interrelated data were listed in table 5. The HRR of PP0 showed a significant increase after ignition up to the peak value (pHRR) and decreased sharply toward the end of burning. When 30 wt% MFT-APP or MFT-APP/THEIC were added into PP, the HRR of the mixure decreased sharply. The pHRR of PP3 and PP6 decreased to 375 kw/$m^2$ and 232 kw/$m^2$, respectively. The values were reduced by 69.7% and 81.2% compared to that of pure PP, respectively. The times to pHRR ($t_{pHRR}$) of PP3 and PP6 were 169s and 192s, respectively.They were significantly delayed in comparison with PP0. For PP0, the largest THR value was 123.7 MJ/$m^2$. In contrast, the curves of PP3 and PP6 showed a much lower value in THR plot, about 116.4 MJ/$m^2$ and 100.7 MJ/$m^2$, respectively. For pSPR and TSP, the relative relationship among PP0, PP3 and PP6 was similar to that of pHRR and THR. At the end of burning, the residual weight of PP3 and PP6 still had 17.4% and 20.7%, respectively. The above results demonstrated that MFT-APP and the intumescent system based on MFT-APP and THEIC could effectively improve the flame retardancy of PP.

( inserting table 5 here)

( inserting table 6 here)

In order to investigate water resistance of the flame retardant composites,

PP/APP/THEIC and PP/MFT-APP/THEIC were soaked in water at 70 $^{o}$C for different time and their flame retardancy properties were tested, including LOI and UL-94 tests. The results were listed in table 6. PP/APP/THEIC only obtained a V-2 rating after 24 hrs, with melt dripping occurred during combustion process. After 48 hrs, no rating could be obtained for it. However, PP/MFT-APP/THEIC could still obtain V-0 rating after 96 hrs soaking time. The results indicated MFT-APP/THEIC has a good water resistant property, the flame retardant durability of PP/MFT-APP/THEIC was improved greatly compared with PP/APP/THEIC composite.

(inserting figure 13 here)

The mechanical properties of flame retardant composites are presented in figure 13, including tensile properties and flexural properties. It can be seen that the addition of APP into PP decreases sharply the tensile strength and flexural strength of PP1, with a falling range about 35.1% and 21.4% respectively. when MFT-APP is added into PP, the falling range is not so much. The falling range for PP2 is only 18.9% and 0% respectively. So there is a improvement of compatibility when MFT-APP is added into PP compared with APP. When THEIC is added into the composites, the situation between PP6 and PP9 is not so obvious. The falling ranges of tensile strength and flexural strength of PP9 are 43.2% and 14.3% respectively. The results for PP6 is 29.7% and 14.2%. We think the reason for the above situation between PP6 and PP9 is that THEIC can react with APP or MFT-APP in the processing. So the superiority of MFT-APP in compatibility can not be shown.

### *3.3 Thermal degradation analysis*

(inserting figure 14 here)

TGA-FTIR spectra were used to analyze the gas produced during the thermal degradation process of polymers. The three-dimensional TGA-FTIR spectrum and characteristic spectra obtained at different temperature of PP6 is shown in Figure 14. In figure 14a, the small band observed at 3,400–4,000 $cm^{-1}$ can be attributed to the O-H vibration of $H_2O$; the intense bands at 2800-3100 $cm^{-1}$ are assigned to saturated hydrocarbons and saturated alkane; another intense bands at 2,300–2,350 $cm^{-1}$ are assigned to $CO_2$; the bands at 2250-2300 $cm^{-1}$ are assigned to CO which is transformed into $CO_2$ with the rising of temperature; the bands at 1600-1900 $cm^{-1}$ are due to the structures containing aromatic rings; the peak near 1370 $cm^{-1}$ is assigned to gase containing the P–O–C structure; the sharp peaks at 930–960 $cm^{-1}$ referred to the N-H vibration of $NH_3$. In figure 14b, FTIR spectra of volatile pyrolysis products evolved at different temperature are shown. There is almost no infrared signal below 200 $^oC$, indicating that the MFT-APP/THEIC mixture do not decompose under this temperature, thus it is thermostable for melting-blend with PP (170–210 $^oC$). With further increasing the temperature, the release of $H_2O$, $CO_2$, and $NH_3$, etc. can be detected. The reason for these gases production is that MFT-APP can release $NH_3$ to form poly(phos-phorus acid) and poly(phosphorus acid) and these acid can react with THEIC to release $H_2O$. When the temperature increased to 400 $^oC$, a maximum signal intensity is observed. These can be explained by that, with increasing temperature, a swollen char is formed and prevented the polymer from decomposing. Afterward, the signal intensity of the pyrolysis products decreased gradually, indicating that the decomposition rate of the composite is slowed down by the promoted char formation. When the temperature above 500 $^oC$, the intensity of $CO_2$ is increasing gradually. The reason may be the promoted char layer is decomposing.

(inserting figure 15 here)

In order to futher analyze chemical structure of the char layer, XPS spectra of $C_{1s}$, $O_{1s}$ for PP6 after combustion is studied. The XPS spectra are shown in figure 15. The $C_{1s}$ spectrum is presented in the Figure 15a. The peaks at 284.6 eV and 285.8 eV are assigned to C-H and C-C in aliphatic species and C-O in ether, hydroxyl groups, C-O-P in hydrocarbonated phosphate, and/or C-N in heterocylic compunds, respectively. For the $O_{1s}$ spectrum (figure 9b), two peaks are found at around 532.5 and 533.5 eV. It is impossible to distinguish inorganic and organic oxygen because the $O_{1s}$ band is structureless. The peaks at 532.5 and 533.5 eV are assigned to =O in carbonyl or phophate groups and –O– in C-O-C, C-O-P, or C-OH groups, respectively. The char in form of these structures for PP6 can effectively prevent the substrate materials from burning, thus leading to an efficient flame retardancy.

## *4 Conclusions*

A microencapsulated ammonium polyphosphate with melamine-formaldehyde-tris(2-hydroxyethyl) isocyanurate resin was successfully prepared by in situ polymerization. The water resistance and thermal stability of MFT-APP was improved greatly compared with APP. When 30 wt% MFT-APP was added into PP, UL-94 V-0 rating was achieved with a LOI value of 32%. To further improve the flame retardancy, THEIC was added into the PP/MFT-APP composites, a remarkable improvement of flame retardation could be found. The maximum LOI values increased to 36% and an excellent swell char layer was formed. The results of cone calorimeter test indicated that the addition of MFT-APP or MFT-APP/THEIC

significantly decreased the HRR, pHRR, THR, pSPR and TSP. The results of water resistance test illustrated that MFT-APP was beneficial for improving the flame durability of PP/IFR composites. The TGA-FTIR and XPS results indicated that PP/MPP/TBM could form a compact and thermostable char residue, which could effectively protect the substrate material from burning. All the results illustrated that microencapsulating APP with this MFT- resin was a promising way to endow the PP/IFR with good water resistance and flame retardancy.

**References**

1. P. Song, Z. Fang, L. Tong, Y. Jin, F. Lu , Effects of metal chelates on a novel oligomeric intumescent flame retardant system for polypropylene. Journal of Analytical and Applied Pyrolysis**,** 82 (2008) 286-291.

2. Y. Liu, C. L. Deng, J. Zhao, J. S. Wang, L. Chen, Y. Z. Wang, An efficiently halogen-free flame-retardant long-glass-fiber-reinforced polypropylene system. Polymer Degradation and Stability **,** 96 (2011), 363-370.

3. H. Yu, Z. Jiang, J. W. Gilman, T. Kashiwagi, J. Liu, R. Song, T. Tang, Promoting carbonization of polypropylene during combustion through synergistic catalysis of a trace of halogenated compounds and $Ni_2O_3$ for improving flame retardancy. Polymer**,** 50 (2009), 6252-6258.

4. S. Bourbigot, Bras. M. Le, S. Duquesne, M. Rochery, Recent advances for intumescent polymers. Macromolecular Materials and Engineering**,** 289 (2004), 499-511.

5. N. Tian, X. Wen, Z. Jiang, J. Gong, Y. Wang, J. Xue, T. Tang, Synergistic Effect between a Novel Char Forming Agent and Ammonium Polyphosphate on Flame Retardancy and Thermal Properties of Polypropylene. Industrial & Engineering Chemistry Research **,** 52 (2013), 10905-10915.

6. G. Camino, L. Costa, L. Trossarelli, Study of the mechanism of intumescence in fire retardant polymers: Part III—Effect of urea on the ammonium polyphosphate-pentaerythritol system. Polymer Degradation and Stability **,** 7 (1984), 221-229.

7. G. Camino, L. Costa, L. Trossarelli, F. Costanzi, A. Pagliari, Study of the mechanism of intumescence in fire retardant polymers: Part VI—Mechanism of ester

formation in ammonium polyphosphate-pentaerythritol mixtures. Polymer Degradation and Stability , 12 (1985), 213-228.

8. G. Camino, L. Costa, G. Martinasso, Intumescent fire-retardant systems. Polymer Degradation and Stability, 23 (1989), 359-376.

9. Y. Chen, Q. Wang , Reaction of melamine phosphate with pentaerythritol and its products for flame retardation of polypropylene. Polymers for Advanced Technologies, 18 (2007), 587-600.

10. G. Camino, L. Costa, L. Trossarelli, Study of the mechanism of intumescence in fire retardant polymers: Part II—Mechanism of action in polypropylene-ammonium polyphosphate-pentaerythritol mixtures. Polymer Degradation and Stability , 7 (1984), 25-31.

11. G. Camino, L. Costa, L. Trossarelli, Study of the mechanism of intumescence in fire retardant polymers: Part I—Thermal degradation of ammonium polyphosphate-pentaerythritol mixtures. Polymer Degradation and Stability, 6 (1984), 243-252.

12. G. Camino, L. Costa, L. Trossarelli,Study of the mechanism of intumescence in fire retardant polymers: Part V—Mechanism of formation of gaseous products in the thermal degradation of ammonium polyphosphate. Polymer Degradation and Stability , 12 (1985), 203-211.

13. M. Chen, Y. Xu, X. Chen, Y. Ma, W. He, J. Yu, Z. Zhang, Thermal stability and combustion behavior of flame-retardant polypropylene with thermoplastic polyurethane-microencapsulated ammonium polyphosphate. High Performance Polymers 2014, 26 (4) 445.

14. C. L. Deng, S. L.Du, J. Zhao, Z. Q.Shen, C. Deng, Y. Z. Wang, An intumescent flame retardant polypropylene system with simultaneously improved flame retardancy and water resistance. Polymer Degradation and Stability **,** 108(2014), 97-107.

15. K. Cao, S. l. Wu, K. l. Wang, Z. Yao, Kinetic Study on Surface Modification of Ammonium Polyphosphate with Melamine. Industrial & Engineering Chemistry Research **,** 50 (2011), 8402-8406.

16. Z. B. Shao, C. Deng, Y. Tan, M. J. Chen, L. Chen, Y. Z.Wang, Flame retardation of polypropylene via a novel intumescent flame retardant: Ethylenediamine-modified ammonium polyphosphate. Polymer Degradation and Stability **,** 106 (2014) 88-96.

17. H. Lin, H. Yan, B. Liu, L. Wei, B. Xu, The influence of KH-550 on properties of ammonium polyphosphate and polypropylene flame retardant composites. Polymer Degradation and Stability **,** 96 (2011), 1382-1388.

18. Lei, Z.; Cao, Y.; Xie, F.; Ren, H., Study on surface modification and flame retardants properties of ammonium polyphosphate for polypropylene. Journal of Applied Polymer Science 2012**,** *124* (1), 781-788.

19. K. Wu, Z. Wang, H. Liang, Microencapsulation of ammonium polyphosphate: preparation, characterization, and its flame retardance in polypropylene. Polymer Composites**,** 29 (2008), 854-860.

20. L. Yang, W. Cheng, J. Zhou, H. Li, X. Wang, X. Chen, Z. Zhang, Effects of microencapsulated APP-II on the microstructure and flame retardancy of PP/APP–II/PER composites. Polymer Degradation and Stability**,** 105 (2014)150-159.

21. K. Wu, L. Song, Z. Wang, Y. Hu, Preparation and characterization of double shell microencapsulated ammonium polyphosphate and its flame retardance in polypropylene. Journal of Polymer Research **,** 16 (2008), 283-294.

22 L. G. Wei, M. L. Xie, X. X. Chai, Synthesis of the cocondensation resin of

THEIC , melamine and phenol-formaldehyde and its application. Engineering Plastics Application, 4(1989), 10-13.

23 W. R. Li, H. L. Zhang, X, P. Liu, H. J. Song, Foam level special tri(2-hydroxyethyl) isocyanuratemodified melamine resin. Thermosetting Resin, *26* (2011), 32-35.

24. H. L. Zhang, X. P. Liu, J. W. Zhang, H, J. Song, Study on foam level THEIC modified melamine resin. Chemical Intermediate**,** 1(2011), 28-30.

25. M. Jimenez, S. Duquesne, S. Bourbigot, Intumescent fire protective coating: Toward a better understanding of their mechanism of action. Thermochimica Acta **,** 449 (2006), 16-26.

26. W. Y. Chen, S. S. Yuan, Y. Sheng, G. S. Liu, Effect of charring agent THEIC on flame retardant properties of polypropylene. Journal of Applied Polymer Science**,** 132 (2015), 33-40.

27. S. S. Yuan, W. Y. Chen, G. S. Liu, Synergistic effect of THEIC-Based charring agent on flame retardant properties of polylactide. Journal of Applied Polymer Science**,** 132 (2015),65-69.

28. W.Y. Chen, G.S. Liu, Flame-retardancy properties of tris(2-hydroxyethyl) isocyanurate based charring agents on polypropylene. Journal of Applied Polymer Science, 2015,132(16):5126-5132.

29. B. Du, Z. Guo, P. A. Song, H. Liu, Z. Fang, Y. Wu, Flame retardant mechanism of organo-bentonite in polypropylene. Applied Clay Science**,** 45 (2009), 178-184.

30. X. Su, Y. Yi, J. Tao, H. Qi, Synergistic effect of zinc hydroxystannate with intumescent flame-retardants on fire retardancy and thermal behavior of polypropylene. Polymer Degradation and Stability**,** 97 (2012), 2128-2135.

31. A. B. Morgan, M. Bundy, Cone calorimeter analysis of UL-94 V-rated plastics. Fire Mater, 31(2007), 257−283.

32. B. Schartel, T. R. Hull, Development of fire-retarded materials interpretation of cone calorimeter data. Fire Mater , 31(2007), 327−354.

33. P. J. Elliot, R. H. Whiteley, A cone calorimeter test for the measurement of flammability properties of insulated wire. Polym. Degrad. Stab, 64(1999), 577−584.

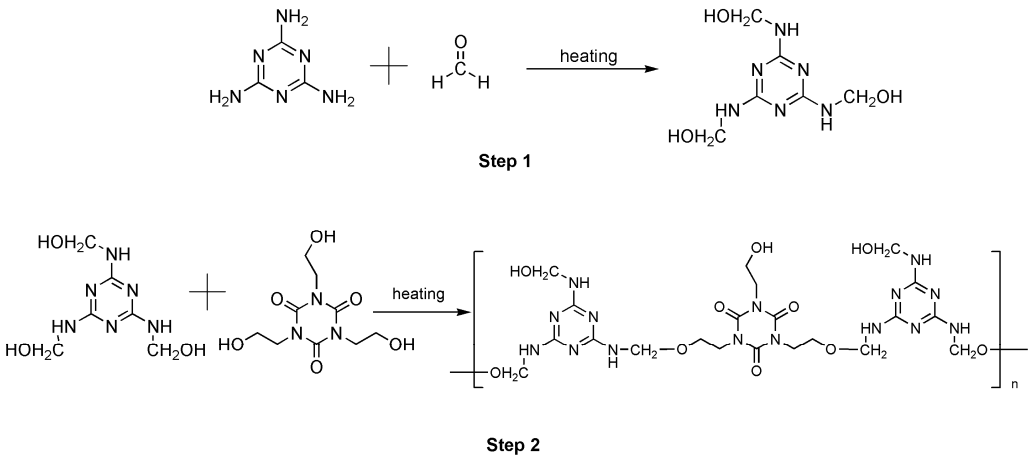


Figure. 1 The reaction scheme of MFT resin pre-polymer

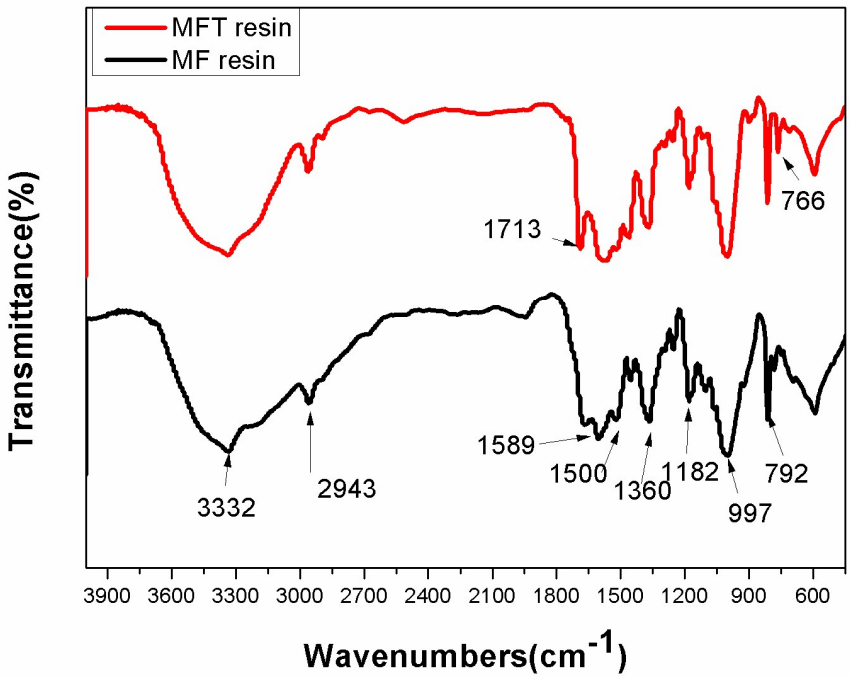


Figure. 2 FTIR spectrum of MF resin and MFT resin

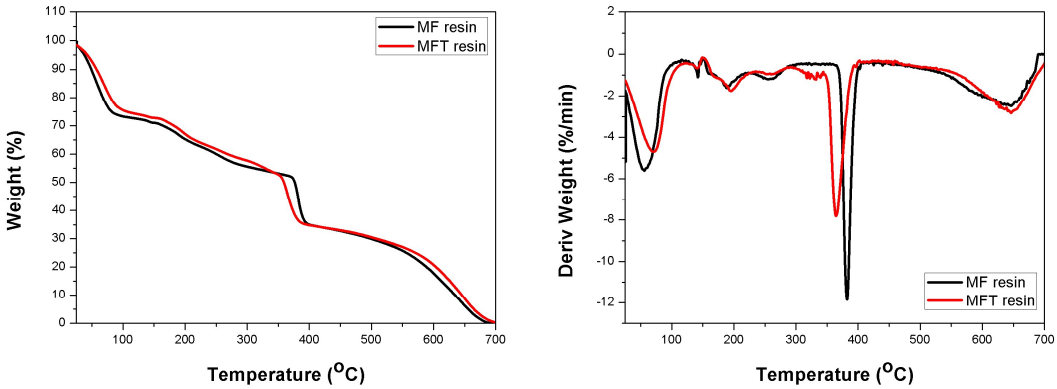


Figure 3. TG and DTG curves of MF and MFT resin

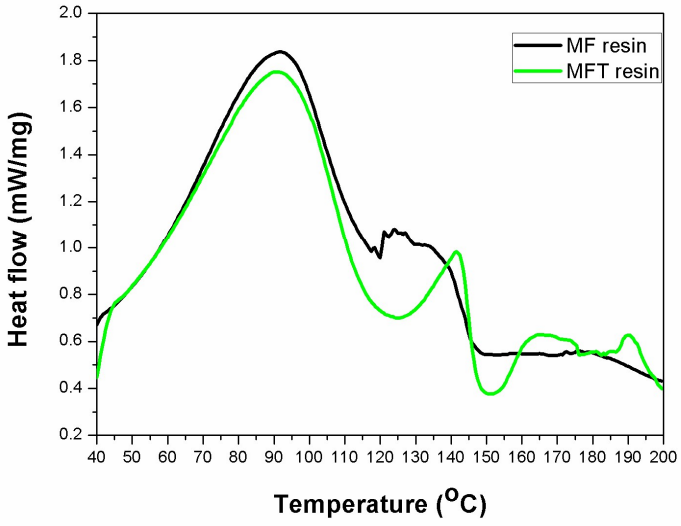


Figure 4. DSC of MF and MFT resin

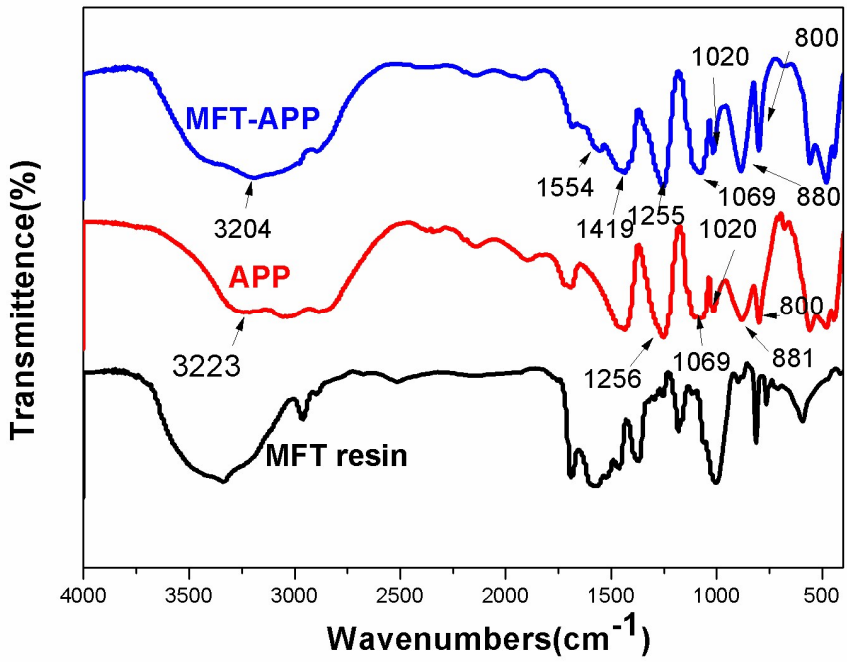


Figure. 5 FTIR spectrum of APP and MFT-APP

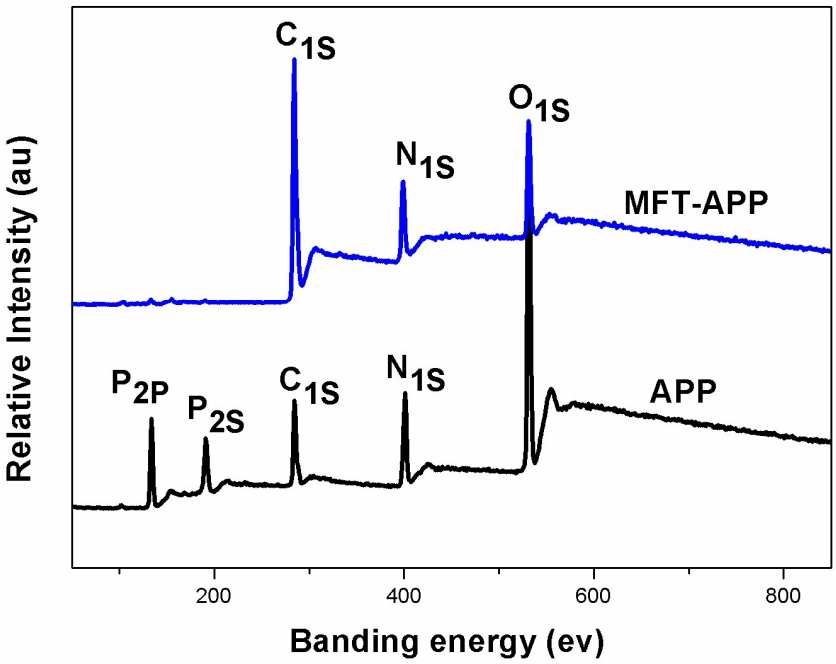


Figure. 6 XPS spectrum of APP and MFT-APP

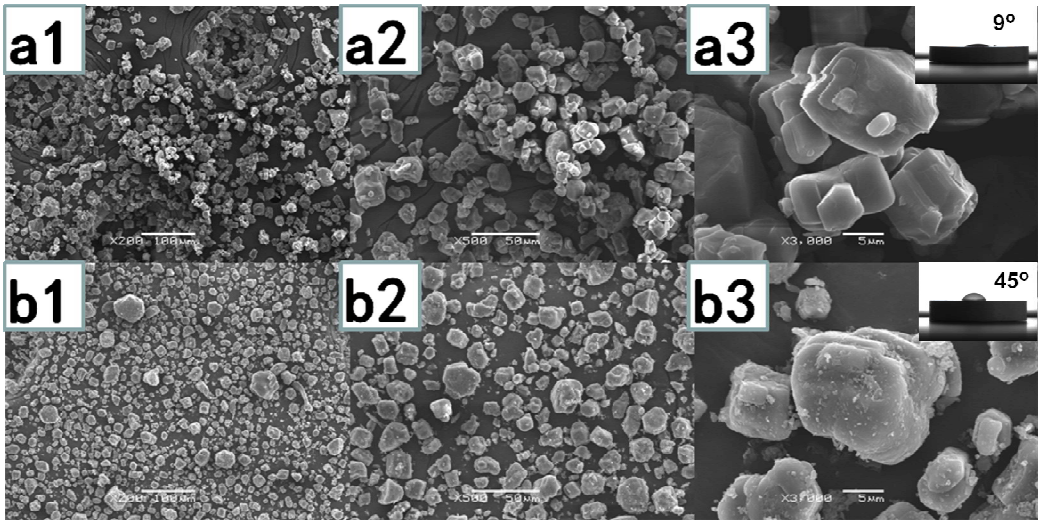


Figure. 7 SEM of APP and MFT-APP

a1. APP ×200, a2. APP×500, a3. APP×3000

b1. MFT-APP×200, b2. MFT-APP×500, b3. MFT-APP×3000

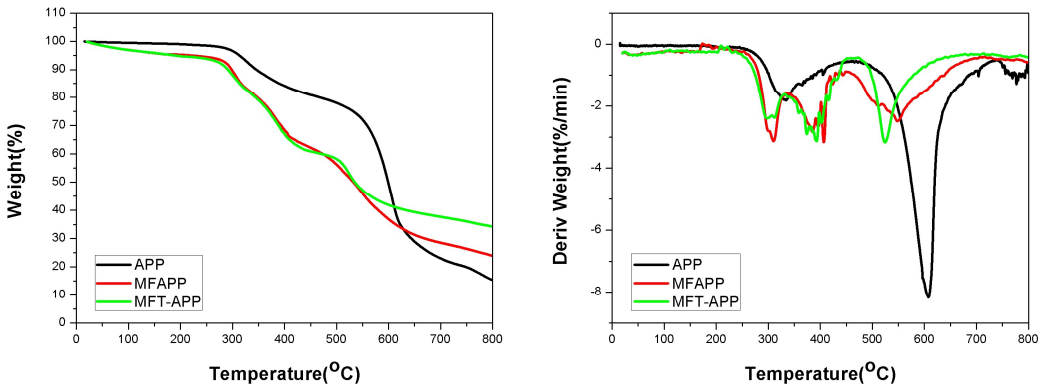


Figure. 8 The TG and DTG curves of APP, MFAPP and MFT-APP

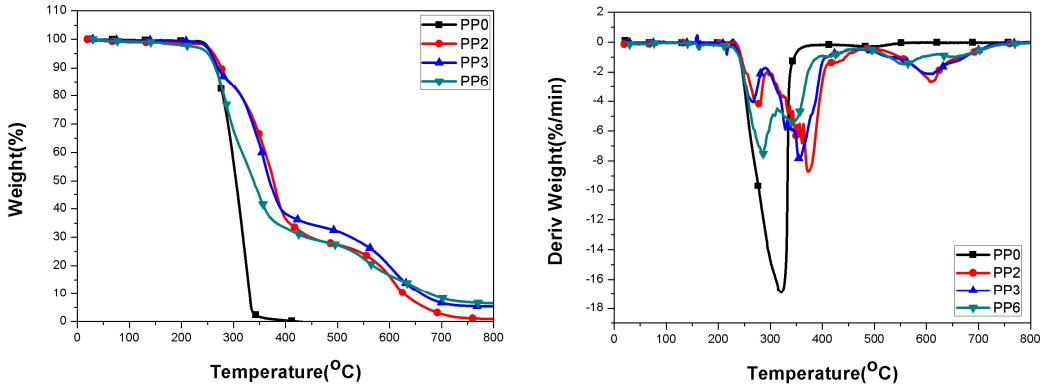


Figure. 9 The TG and DTG curves of PP0, PP2, PP3 and PP6

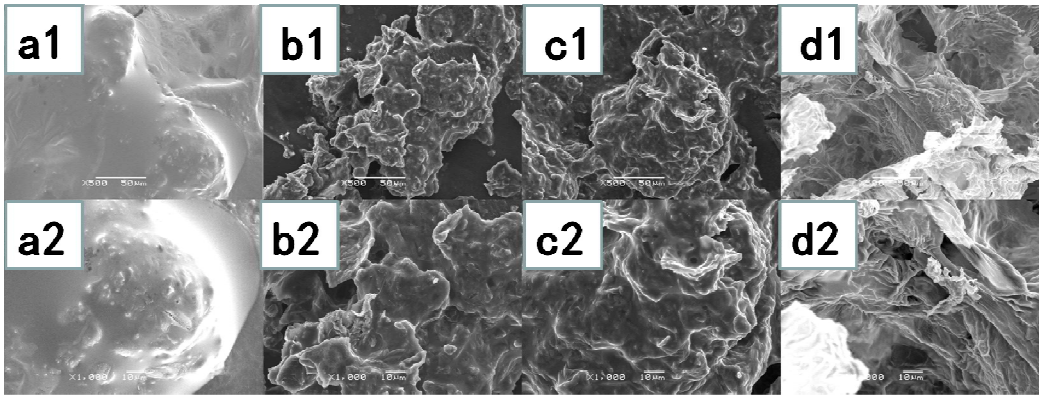


Figure 10. SEM image of the char from PP1, PP2, PP3 and PP6

a1. PP1×500, a2. PP1×1000

b1. PP2×500, b2. PP2×1000

c1. PP3×500, c2. PP3×1000

d1. PP6×500, d2. PP6×1000

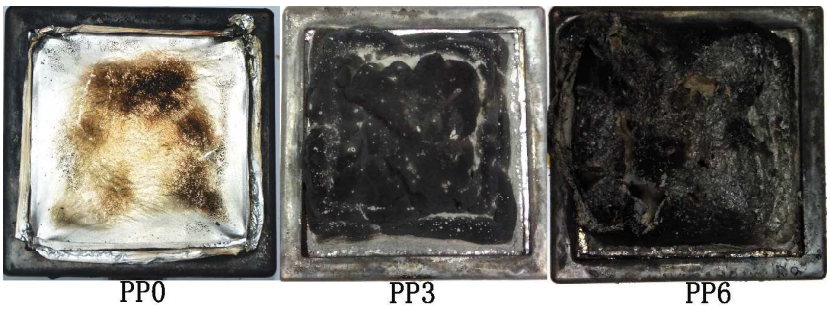


Figure 11. Digital photographs of residues for PP0, PP3 and PP6 after cone calorimeter test

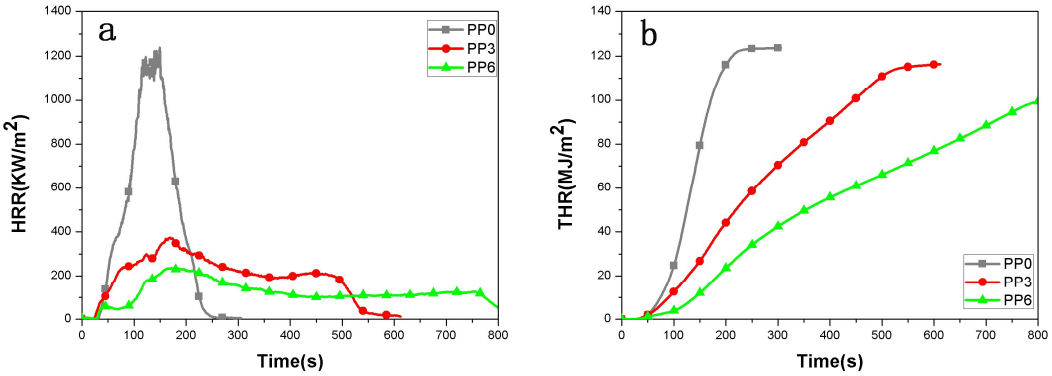


Figure 12. Cone calorimeter test curves of PP0, PP3 and PP6

a: heat release rate curves (HRR) b: total heat release curves (THR)

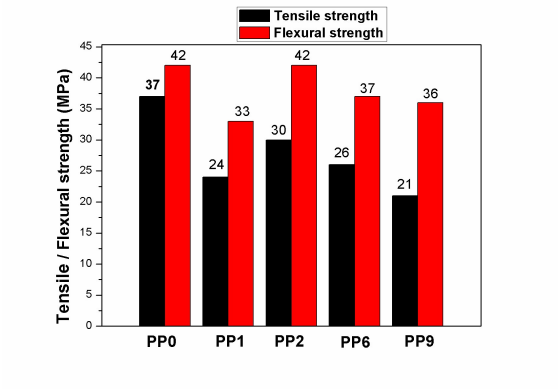


Figure 13. The mechanical properties of PP0, PP1, PP2, PP6 and PP9

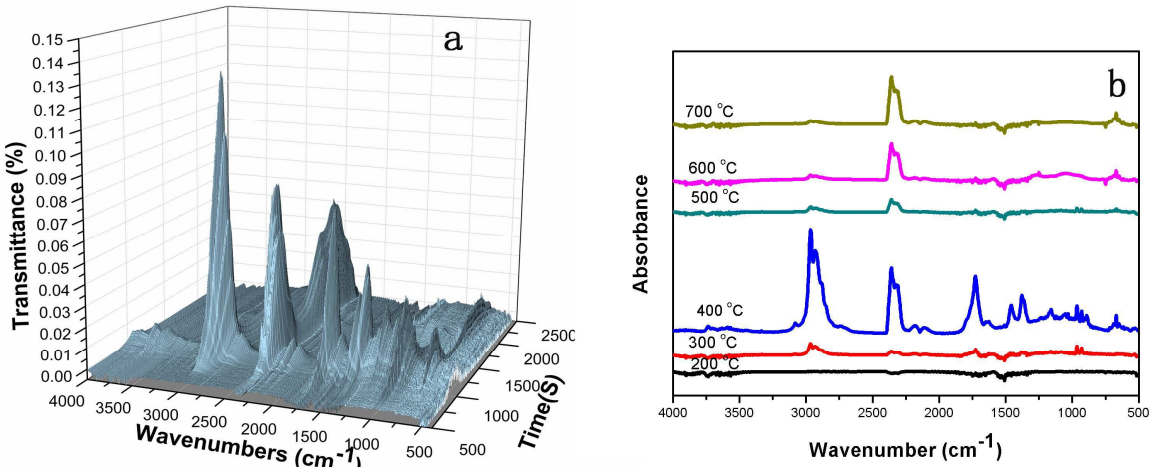


Figure 14. TGA-FTIR spectra of pyrolysis products during the thermal degradation of PP6

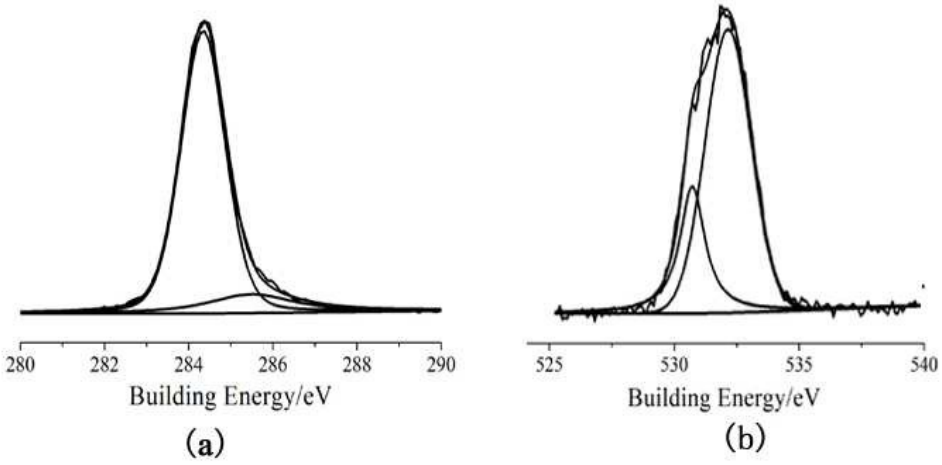


Figure 15. (a) C1s and (b) O1s XPS spectra of the residue of PP6

Table 1. Solubility of APP and MFT-APP

| Sample | Solubility ( 100 g/ml $H_2O$ ) |
|---|---|
| APP | 0.55 |
| MFT-APP | 0.30 |

Table 2. The data of TG and DTG test of APP, MFAPP and MFT-APP

| Sample | $T_{5\%}$ /℃ | $T_{max1}$ /℃ | $T_{max2}$ /℃ | $T_{max3}$ /℃ | $U_{max}$ %/min | Residual 600℃/% | 700℃/% | 800℃/% |
|---|---|---|---|---|---|---|---|---|
| APP | 320.4 | 330 | ---- | 607 | -8.13 | 49.2 | 23 | 14.5 |
| MFAPP | 199.8 | 310 | 405 | 549 | -3.23 | 36.9 | 29.2 | 24.2 |
| MFT-APP | 199.8 | 308 | 391 | 524 | -3.19 | 42.2 | 37.6 | 34.9 |

Table 3. The LOI and UL-94 test results of the samples

| Sample | PP (%) | APP (%) | MFAPP (%) | MFT-APP (%) | THEIC (%) | MFT-APP:THEIC | LOI （%） | UL-94 |
|---|---|---|---|---|---|---|---|---|
| PP0 | 100 | 0 | 0 | 0 | 0 | 0 | 17.8 | N.R |
| PP1 | 70 | 30 | 0 | 0 | 0 | 0 | 21 | N.R |
| PP2 | 70 | 0 | 30 | 0 | 0 | 0 | 30.5 | N.R |
| PP3 | 70 | 0 | 0 | 30 | 0 | 0 | 32 | V-0 |
| PP4 | 70 | 0 | 0 | 15 | 15 | 1 | ---- | ---- |
| PP5 | 70 | 0 | 0 | 20 | 10 | 2 | 35 | V-0 |
| PP6 | 70 | 0 | 0 | 22.5 | 7.5 | 3 | 36 | V-0 |
| PP7 | 70 | 0 | 0 | 25 | 5 | 5 | 35.5 | V-0 |
| PP8 | 70 | 0 | 0 | 27 | 3 | 9 | 34 | V-0 |
| PP9 | 70 | 22.5 | 0 | 0 | 7.5 | 0 | 34.3 | V-0 |
| PP10 | 75 | 0 | 0 | 12.5 | 12.5 | 1 | ---- | ---- |
| PP11 | 75 | 0 | 0 | 16.7 | 8.3 | 2 | 32.5 | V-0 |
| PP12 | 75 | 0 | 0 | 18.75 | 6.25 | 3 | 33 | V-0 |
| PP13 | 75 | 0 | 0 | 20.83 | 4.17 | 5 | 32 | V-0 |
| PP14 | 75 | 0 | 0 | 22.5 | 2.5 | 9 | 31 | V-0 |

N.R= No rating

Table 4. The data of TG and DTG test of PP0, PP2, PP3 and PP6

| Sample | $T_{5\%}$ /℃ | $T_{max1}$ /℃ | $T_{max2}$ /℃ | $T_{max3}$ /℃ | $U_{max}$ %/min | Residual 600℃/% | 700℃/% | 800℃/% |
|---|---|---|---|---|---|---|---|---|
| PP0 | 257.6 | 322.5 | ---- | ---- | -16.95 | 0 | 0 | 0 |
| PP2 | 261 | 276 | 370 | 611 | -9.75 | 16.3 | 2.69 | 0.88 |
| PP3 | 258.5 | 266 | 357 | 607 | -7.77 | 19.8 | 6.72 | 5.42 |
| PP6 | 250.9 | 287 | 339 | 569 | -7.5 | 16.7 | 8.44 | 6.5 |

Table 5. Combustion parameters obtained from cone calorimeter

| Sample | TTI (s) | pHRR( kw/$m^2$) | $t_{pHRR}$( s) | THR( MJ/$m^2$) | pSPR( $m^2$/s) | TSP( $m^2$) | Residue(%) |
|---|---|---|---|---|---|---|---|
| PP0 | 33 | 1238 | 149 | 123.7 | 0.154 | 15.78 | 0 |
| PP3 | 24 | 375 | 169 | 116.4 | 0.058 | 14.45 | 17.4 |
| PP6 | 28 | 232 | 192 | 100.7 | 0.04 | 13.38 | 20.7 |

Table 6. Effect of water soaking time on LOI value of PP/IFR composites

| Water treated time | PP/APP/THEIC | | PP/MFT-APP/THEIC | |
|---|---|---|---|---|
| | UL-94 V-rank | LOI | UL-94 V-rank | LOI |
| 24h | V-2 | 30.2% | V-0 | 33% |
| 48h | NR | 28.5% | V-0 | 32% |
| 72h | NR | 27.5% | V-0 | 32% |
| 96h | NR | 26.9% | V-0 | 31% |